

# Inhibition of Na<sup>+</sup> Current by Imipramine and Related Compounds: Different Binding Kinetics as an Inactivation Stabilizer and as an Open Channel Blocker

YA-CHIN YANG, and CHUNG-CHIN KUO

Department of Physiology, National Taiwan University College of Medicine (Y.-C.Y., C.-C.K.); and Department of Neurology, National Taiwan University Hospital (C.-C.K.)

Received April 1, 2002; accepted July 22, 2002

This article is available online at <http://molpharm.aspetjournals.org>

## ABSTRACT

Use-dependent block of Na<sup>+</sup> channels plays an important role in the action of many medications, including the anticonvulsants phenytoin, carbamazepine, and lamotrigine. These anticonvulsants all slowly yet selectively bind to a common receptor site in inactivated but not resting Na<sup>+</sup> channels, constituting the molecular basis of the use-dependent block. However, it remains unclear what channel gating process “makes” the receptor, where the receptor is located, and how the slow drug binding rate (to the inactivated channels) is contrived. Imipramine has a diphenyl structural motif almost identical to that in carbamazepine (a dibenzazepine tricyclic compound), as well as a tertiary amine chain similar to that in many prototypical local anesthetics, and has also been reported to inhibit Na<sup>+</sup> channels in a use-dependent fashion. We found that imipra-

mine selectively binds to the inactivated (dissociation constant ~1.3 μM) rather than the resting Na<sup>+</sup> channels (dissociation constant >130 μM). Moreover, imipramine rapidly blocks open Na<sup>+</sup> channels, with a binding rate ~70-fold faster than its binding to the inactivated channels. Similarly, carbamazepine and diphenhydramine are open Na<sup>+</sup> channel blockers with faster binding rates to the open than to the inactivated channels. These findings indicate that the anticonvulsant receptor responsible for the use-dependent block of Na<sup>+</sup> channels is located in or near the pore (most likely in the pore mouth) and is made suitable for drug binding during channel activation. The receptor, however, continually changes its conformation in the subsequent gating process, causing the slower drug binding rates to the inactivated Na<sup>+</sup> channels.

Use-dependent inhibition of neuronal Na<sup>+</sup> currents is an important pharmacological phenomenon, which plays an essential role in the mechanism of action of many widely prescribed non-sedative anticonvulsants (e.g., phenytoin, carbamazepine, and lamotrigine) and prototypical local anesthetics (lidocaine and other “caines”). The molecular basis of the use-dependent inhibition is two-fold. In terms of steady-state effect, these anticonvulsants and local anesthetics show much higher affinity to the inactivated than to the resting Na<sup>+</sup> channels and thus selectively bind to the former rather than the latter (Bean et al., 1983; Matsuki et al., 1984; Butterworth and Strichartz, 1990; Kuo and Bean, 1994; Xie et al., 1995; Kuo and Lu, 1997; Kuo et al., 1997). In terms of kinetic attributes, these drugs have slow binding rates onto the inactivated Na<sup>+</sup> channel during depolarization, so that binding and “stabilization” of the inactivated Na<sup>+</sup> channels do not reach the steady state in one short depolarizing pulse but are gradually accumulated with repeated pulses (and thus “use-dependent” inhibition of the Na<sup>+</sup> current). The binding rates of the foregoing anticonvulsants onto the inactivated Na<sup>+</sup> channels, for example, are only ~10,000 to

40,000 M<sup>-1</sup>s<sup>-1</sup> in rat hippocampal neurons (Kuo and Bean, 1994; Kuo et al., 1997; Kuo and Lu, 1997).

Recently, we have shown that phenytoin, carbamazepine, and lamotrigine probably bind to the same receptor site in the inactivated Na<sup>+</sup> channel, most likely with the diphenyl motif as the major binding ligands (Fig. 1A; Kuo, 1998a; Kuo et al., 2000). A tertiary amine chain, if present in the appropriate position, may also contribute to drug binding (Kuo et al., 2000). The local anesthetics, which usually have only one phenyl group with a tertiary amine chain, may have their receptor area overlapping with the anticonvulsant receptor because some point mutations of the Na<sup>+</sup> channel could decrease the binding affinity of both groups of drugs (Ragsdale et al., 1996; Yarov-Yarovoy et al., 2001). However, there is still a possibility that the two groups of drugs have separate but allosterically linked receptors with their conformational changes controlled by the same gating process of the channel (Li et al., 1999).

Because inactivation is coupled to activation in Na<sup>+</sup> channels, the resting channel usually is activated and then inactivated upon membrane depolarization. Does channel activation or inactivation “make” the anticonvulsant receptor, which is present in the inactivated but not in the resting channels? The single Na<sup>+</sup> channel open time was shortened

This work is supported by grant NTUH.S90-1500-36 from the National Taiwan University Hospital, and grant NHRI-EX91-9105NN from the National Institute of Health, Taiwan.

by phenytoin (Quandt, 1988) but not local anesthetic lidocaine (Benz and Kohlhardt, 1992; Balser et al., 1996), suggesting that phenytoin is an open channel blocker but lidocaine is not; consequently, lidocaine might be chiefly an inactivation stabilizer (e.g., Bennett et al., 1995; Balser et al., 1996). However, the foregoing experiments were performed in mutant or chemically modified Na<sup>+</sup> channels deficient of fast inactivation, and there is always a concern that the drug receptor may also be directly or allosterically altered by the modification procedures (e.g., Bennett et al., 1995; Li et al., 1999). On the other hand, lidocaine was proposed to block open Na<sup>+</sup> channel pore or stabilize activated channel conformation based on more indirect evidences such as the biphasic

kinetics in the development of or recovery from drug action (e.g., Matsubara et al., 1987; Clarkson et al., 1988) and slowing of Na<sup>+</sup> channel repriming (from inactivation) without slowing of recovery of the fast-inactivation gate itself (Vedantham and Cannon, 1999). It is thus unsettled whether the receptor(s) for anticonvulsants and/or local anesthetics are well developed in the open native Na<sup>+</sup> channel, whether the receptor(s) continue to have significant conformational changes after channel activation, and whether binding of these drugs blocks ion permeation through the pore. Besides, we have noted that the drug binding kinetics may play an important role in the use-dependent inhibitory effect, but it remains obscure whether any structural feature of a drug could be correlated with its binding kinetics.

In an attempt to clarify the foregoing points, we studied the effect of imipramine and other related compounds on neuronal Na<sup>+</sup> channels in detail. Imipramine is a commonly prescribed antidepressant that has been shown to inhibit Na<sup>+</sup> currents and the inhibitory effect is stronger with higher frequency of depolarizing pulses or more depolarized holding potentials (Ogata and Narahashi, 1989; Bolotina et al., 1992; Kuo et al., 2000). Structurally, imipramine contains a diphenyl motif and a tertiary amine chain. Moreover, the two phenyl groups in imipramine share essentially the same three-dimensional arrangement with those in the dibenzazepine tricyclic motif in carbamazepine (Fig. 1A). In this study, we show that imipramine, carbamazepine, and diphenhydramine all block open Na<sup>+</sup> channels, and all have different binding kinetics to the open and to the inactivated channels. Also, the dibenzazepine tricyclic motif probably holds the two benzene rings in the most favorable conformation for drug binding to the anticonvulsant receptor, which is formed during channel activation yet changes its conformation further in the subsequent gating process.

## Materials and Methods

**Cell Preparation.** Coronal slices of the whole brain were prepared from 7- to 14-day-old Long-Evans rats. The CA1 region was dissected from the slices and cut into small chunks. After treatment for 5–10 min in dissociation medium (82 mM Na<sub>2</sub>SO<sub>4</sub>, 30 mM K<sub>2</sub>SO<sub>4</sub>, 3 mM MgCl<sub>2</sub>, 5 mM HEPES, 0.001% phenol red indicator, and 0.5 mg/ml type XI trypsin, pH 7.4, 37°C), tissue chunks were transferred to dissociation medium containing no trypsin but 1 mg/ml bovine serum albumin and 1 mg/ml type II-S trypsin inhibitor (Sigma, St. Louis, MO). Each time that cells were needed, two to three chunks were picked and triturated to release single neurons.

**Whole-Cell Recording.** The dissociated neurons were put in a recording chamber containing Tyrode's solution (150 mM NaCl, 4 mM KCl, 2 mM MgCl<sub>2</sub>, 2 mM CaCl<sub>2</sub>, and 10 mM HEPES, pH 7.4). Whole-cell voltage clamp recordings were obtained using pipettes pulled from borosilicate micropipettes (OD 1.55–1.60 mm; Hilgenberg Inc., Malsfeld, Germany), fire polished, and coated with Sylgard (Dow-Corning, Midland, MI). The pipette resistance was 1 to 2 MΩ when filled with the internal solution containing 75 mM CsCl, 75 mM CsF, 2.5 mM MgCl<sub>2</sub>, 5 mM HEPES, 2.5 mM EGTA, pH adjusted to 7.4 by CsOH. Seal was formed and the whole-cell configuration obtained in Tyrode's solution. The cell was then lifted from the bottom of the chamber and moved in front of an array of flow pipes (Microcapillary; Hilgenberg Inc., Germany; content, 1 μl; length, 64 mm) emitting either control or drug-containing external recording solutions. Imipramine and diphenhydramine were dissolved in water, carbamazepine, and lamotrigine were dissolved in dimethyl sulfoxide to make 100 mM stock solutions, which were then diluted into

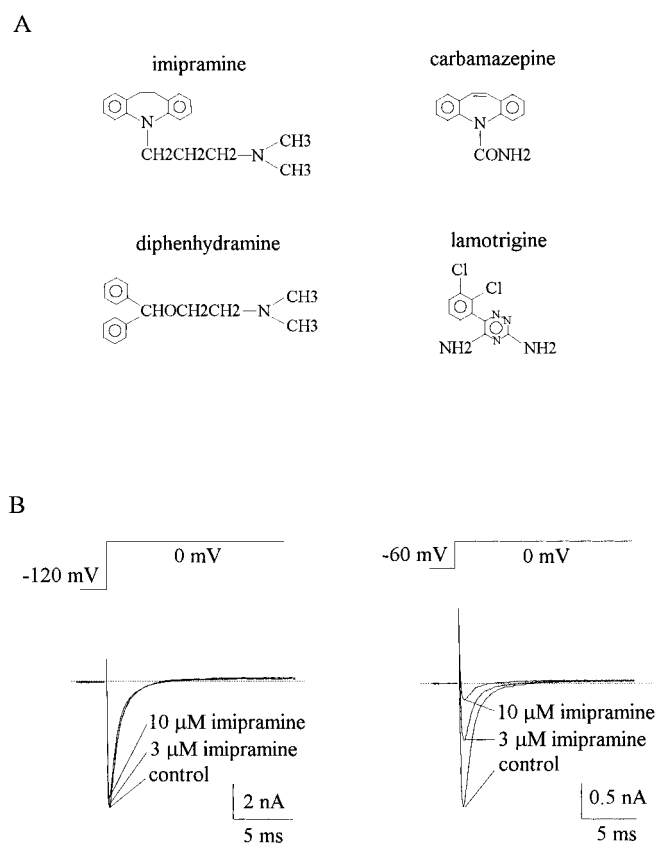


**Fig. 1.** Chemical formulae of the drugs and inhibition of Na<sup>+</sup> currents by imipramine. A, chemical formulae of imipramine, carbamazepine, diphenhydramine, and lamotrigine. These compounds all contain the diphenyl structural motif, which is composed of two phenyl groups separated by a center-to-center distance of ~5 Å and a stem-bond angle of ~110° (Kuo et al., 2000) and probably serves as the major binding ligands to a common anticonvulsant receptor site in the extracellular side of the Na<sup>+</sup> channel (Kuo, 1998a). The diphenyl motifs in imipramine and carbamazepine even have the same torsion angles and are thus essentially the same in the three-dimensional structure. In contrast, the diphenyl motifs in imipramine, diphenhydramine, and lamotrigine all have quite different torsion angles (Kuo et al., 2000). However, imipramine and diphenhydramine both contain a similar tertiary amine chain, which is not present in carbamazepine. B, Na<sup>+</sup> currents in control, 3 μM, or 10 μM imipramine were recorded in a neuron. The cell was held at -120 mV and stepped to 0 mV for 17 ms every second. Imipramine (3 and 10 μM) produce only equivocal and mild inhibition of the Na<sup>+</sup> current, respectively. The same experiment was repeated in the same cell except that the holding potential was changed to -60 mV (right). The currents are much smaller than those on the left but are scaled to the same size for better comparison (note the difference in the vertical scale bars). In contrast to the findings on the left, 3 to 10 μM imipramine here shows a remarkable inhibitory effect on the Na<sup>+</sup> current. The dotted line indicates zero current level in both.

Tyrode's solution to attain the final concentrations desired. The final concentration of dimethyl sulfoxide (0.3% or less) was not found to have detectable effect on  $\text{Na}^+$  currents. Lamotrigine was a kind gift from Wellcome Foundation (Kent, England), and the other drugs were purchased from Sigma. Currents were recorded at room temperature ( $\sim 25^\circ\text{C}$ ) with an Axoclamp 200A amplifier, filtered at 5 kHz with four-pole Bessel filter, digitized at 50- to 200- $\mu\text{s}$  intervals, and stored using a Digidata-1200 analog/digital interface as well as the pCLAMP software (Axon Instruments, Union City, CA).

**Molecular Biology.** The plasmid pNa200 encoding the rat brain type IIA (RIIA)  $\text{Na}^+$  channel  $\alpha$  subunit was a kind gift from Dr. Alan L. Goldin (Department of Microbiology and Molecular Genetics, University of California, Irvine, CA). The plasmid also provides the *Xenopus laevis*- $\beta$ -globulin untranslated sequence that improves expression of exogenous proteins in oocytes. The pNa200 has unique *Xho*I and *Not*I restriction sites, between which is the coding region containing another unique *Bgl*II site. To optimize the mutagenesis process, we first divided the entire coding region into two subfragments (the *Xho*I-*Bgl*II and *Bgl*II-*Not*I subfragments, each about 3~4 kb in size) and subcloned each subfragment into another small and easily growing vector pBSTA (also kindly provided by Dr. A. L. Goldin). F1489Q point mutation (West et al., 1992) was done with the [*Bgl*II-*Not*I]-pBSTA plasmid DNA template and polymerase chain reaction-based method (QuikChange mutagenesis kit; Stratagene, LA Jolla, CA), and was verified by DNA sequencing. The mutation-containing subfragment from [*Bgl*II-*Not*I]-pBSTA plasmid was then excised and transferred back into pNa200 expression vector. DNA sequencing was performed again at this moment and two independent clones were tested to exclude effects of inadvertent mutations. The full-length cRNA transcript was synthesized from the pNa200 containing the F1489Q mutation using the T7 mMES-SAGE mMACHINE transcription kit (Ambion, Austin, TX). The defolliculated *X. laevis* oocytes (stage V-VI) were then injected with the cRNA transcript and maintained at  $18^\circ\text{C}$  for 1 to 7 days for electrophysiological studies.

**Intracellular Recording.** Macroscopic F1489Q mutant  $\text{Na}^+$  current was examined by two-microelectrode voltage-clamp recordings in oocytes. During recording, the oocyte in the chamber was continuously perfused with ND-96 solution (96 mM NaCl, 2 mM KCl, 1 mM  $\text{MgCl}_2$ , 1.8 mM  $\text{CaCl}_2$ , 5 mM HEPES, pH 7.6) which did or did not contain the aforementioned drugs. Both voltage-sensing and current-passing electrodes were filled with 3 M KCl and had resistance of 0.1 to 0.8 M $\Omega$ . Membrane potential was controlled by a two-electrode voltage-clamp amplifier with a virtual ground circuit (model OC-725C; Warner Instrument, Hamden, CT). Currents were recorded at room temperature ( $\sim 25^\circ\text{C}$ ), filtered at 5 kHz, digitized at 20- to 100- $\mu\text{s}$  intervals, and stored using a Digidata-1200 analog/digital interface as well as the pCLAMP software (Axon Instruments). All statistics in this study are given as mean  $\pm$  S.E.M.

## Results

**Different Inhibitory Effect of Imipramine on  $\text{Na}^+$  Currents Elicited from Different Holding Potentials.** Figure 1B shows the effect of imipramine on neuronal  $\text{Na}^+$  currents. Imipramine (3  $\mu\text{M}$ ) has barely any inhibitory effect on the  $\text{Na}^+$  current elicited from a holding potential of  $-120$  mV, and even 10  $\mu\text{M}$  imipramine produces only slight inhibition. On the other hand, imipramine has much stronger inhibitory effect on the  $\text{Na}^+$  current elicited from more positive holding potentials such as  $-60$  mV, where 3  $\mu\text{M}$  imipramine inhibits more than half of the current, and most of the current is inhibited by 10  $\mu\text{M}$  imipramine. It is evident that the inhibitory effect of imipramine on the  $\text{Na}^+$  current is very much dependent on the holding potentials.

**Dual Effect of Imipramine on  $\text{Na}^+$  Currents at Concentrations Higher Than 30  $\mu\text{M}$ .** The inhibitory effect of

imipramine on  $\text{Na}^+$  currents elicited from different holding potentials are plotted in Fig. 2, where the data are fitted by one-to-one binding curves. If one fits the whole set of data (1

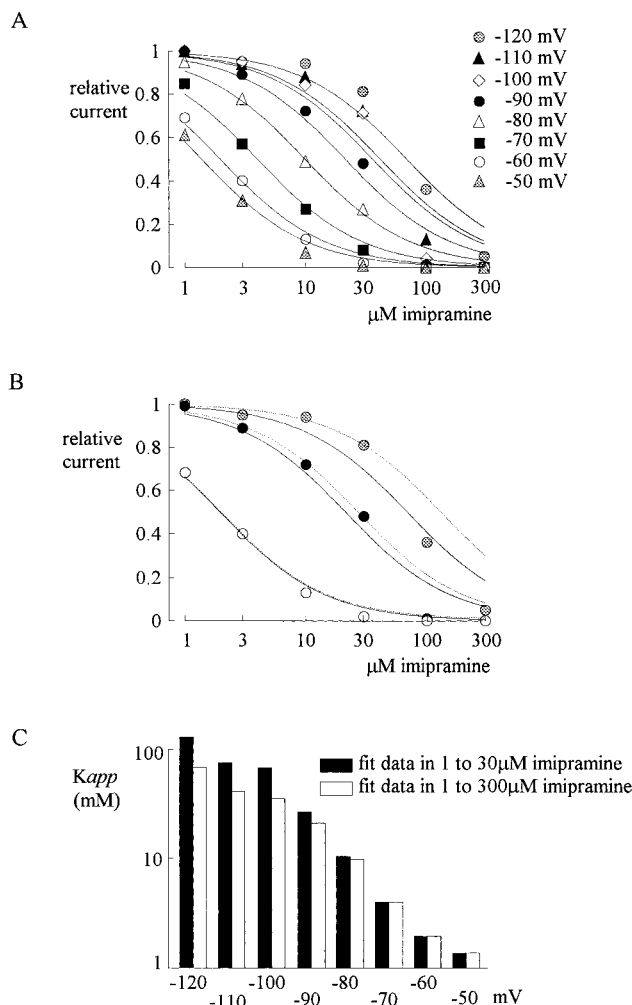
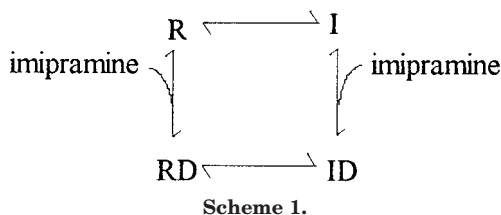


**Fig. 2.** Apparent dissociation constants between imipramine and the  $\text{Na}^+$  channel. A, dose-response curves for inhibition of  $\text{Na}^+$  currents by 1 to 300  $\mu\text{M}$  imipramine at different holding potentials ( $-50$  to  $-120$  mV). The test pulse protocol is the same as that described in Fig. 1. The peak currents in the presence of imipramine are normalized to the peak current in control at each holding potential to give the relative currents, which are plotted against the concentration of imipramine (imipramine) in a semilogarithmic scale. Each data point represents the mean from three to seven cells. The S.E.M. are in general smaller than 10 to 20% of the means and are not shown. The lines are fits to each set of data based on one-to-one binding reactions and are of the form: relative current =  $1/[1 + (\text{imipramine}/K_{app})]$ , where  $K_{app}$  stands for the apparent dissociation constant and are 68.4, 41.5, 35.8, 21.2, 9.9, 4.0, 1.96, and 1.37  $\mu\text{M}$  at holding potentials  $-120$ ,  $-110$ ,  $-100$ ,  $-90$ ,  $-80$ ,  $-70$ ,  $-60$ , and  $-50$  mV, respectively. B, a closer examination of the fitting results in part A reveals that the data points at each holding potential are not very well described by the foregoing one-to-one binding curves. The data points of 100 and 300  $\mu\text{M}$  imipramine tend to fall below the fits. Three sets of data at holding potentials  $-120$ ,  $-90$ , and  $-60$  mV along with the fitting curves in part A (solid lines) are replotted here for a better illustration of this point. If one fits only the data points in low concentrations (1 to 30  $\mu\text{M}$ ) of imipramine, the fitting curves could very well describe the data (the dotted lines), yet the residual currents in 100 and 300  $\mu\text{M}$  imipramine are even smaller than the predicted values by the dotted lines. The  $K_{app}$  from the dotted lines are 130, 27.0, and 1.96  $\mu\text{M}$  at holding potentials  $-120$ ,  $-90$ , and  $-60$  mV, respectively. C, at each holding potential, the  $K_{app}$  from different fitting ranges in parts A and B are plotted together for comparison. The  $K_{app}$  generally becomes smaller as the holding potential becomes more positive, so is the difference between  $K_{app}$  from the two fitting ranges.



to 300  $\mu\text{M}$  imipramine), Na<sup>+</sup> currents are inhibited by imipramine with an apparent dissociation constant ( $K_{\text{app}}$ ) of  $\sim 68$   $\mu\text{M}$  when the holding potential is  $-120$  mV. The  $K_{\text{app}}$  steadily decreases with more positive holding potentials, and becomes  $\sim 1.4$   $\mu\text{M}$  when the holding potential is  $-50$  mV (Fig. 2A). However, a closer examination reveals that these fits do not well describe the data. There is clearly a tendency for the data points in 100 and 300  $\mu\text{M}$  imipramine to fall below the predicted values of the fitting lines. In Fig. 2B, the one-to-one binding curves are fitted only to the data points in low concentrations of imipramine. The new fits reasonably describe the data points in 1 to 30  $\mu\text{M}$  imipramine, supporting the presumption of one-to-one binding, at least in this concentration range. Deviation of the data points in 100 and 300  $\mu\text{M}$  imipramine from the predicted values is even more evident with the new fits, except for the currents elicited from rather positive holding potentials ( $-70$  to  $-50$  mV) where there is almost no residual Na<sup>+</sup> current in 100 and 300  $\mu\text{M}$  imipramine anyway. Figure 2C shows that the  $K_{\text{app}}$  at a holding potential of  $-120$  mV is evidently different between the results in Fig. 2, A and B (126 versus 68  $\mu\text{M}$ ), but the difference gradually decreases with more positive holding potentials. These findings suggest that the inhibition of Na<sup>+</sup> current by imipramine could be explained with a one-to-one binding process if the imipramine concentration is low (30  $\mu\text{M}$  or lower). However, an additional action of imipramine on the Na<sup>+</sup> current becomes too manifest to be disregarded in higher concentrations of the drug. The essential feature of this additional inhibitory action is its concentration dependence, because it would produce significant effect only when imipramine concentration is higher than 30 to 100  $\mu\text{M}$ . The  $K_{\text{app}}$  obtained in Fig. 2B thus should be the better estimate of the binding affinity of imipramine underlying the inhibitory effect that is fully evident even in very low concentrations of imipramine.

Because most Na<sup>+</sup> channels would be in the inactivated and resting states at holding potentials of  $-50$  mV and  $-120$  mV, respectively (see the control inactivation curves in Fig. 3A below), the foregoing inhibitory effect, which is evident even in low concentrations of imipramine, is most likely caused by differential affinity of imipramine to the inactivated and the resting states of the Na<sup>+</sup> channel, just like the cases of phenytoin, carbamazepine, and lamotrigine (Kuo and Bean, 1994; Kuo et al., 1997; Kuo and Lu, 1997). A more quantitative treatment of the effect of selective binding of imipramine to the inactivated state can be given with this scheme:



where R and I are the resting and inactivated states of the channel, and RD and ID are the imipramine-bound resting and inactivated states, respectively. The activated (open) state is omitted here because most activated Na<sup>+</sup> channels would be quickly inactivated, and thus for a steady-state condition one may just consider R and I states for simplicity.

According to this scheme, at a particular holding potential the fraction of channels in state R (the channels that can be activated, or therefore the current that could be elicited upon membrane depolarization) would be reduced by imipramine

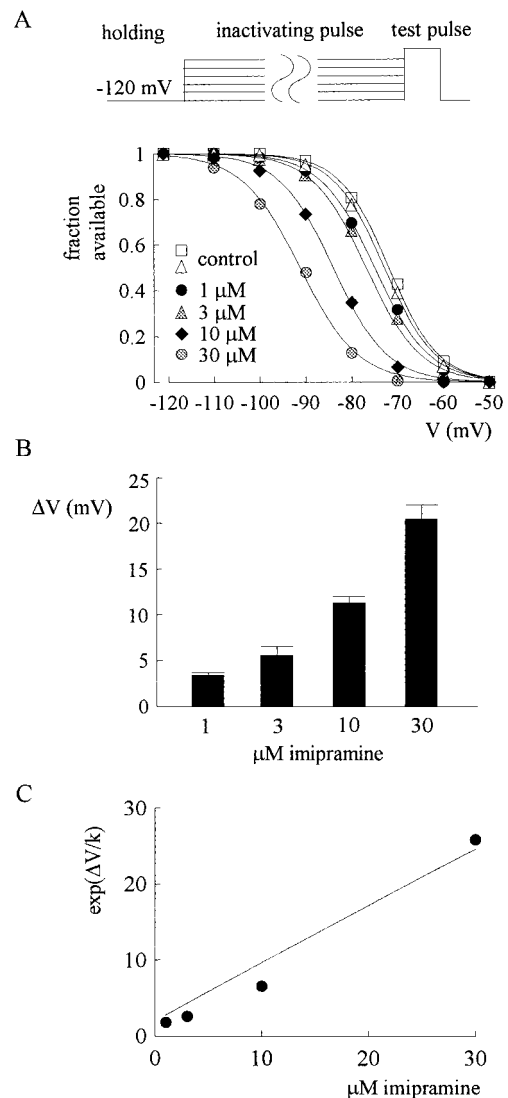


**Fig. 3.** Shift of the inactivation curve by imipramine. A, the cell was held at  $-120$  mV and stepped every 15 s to the inactivating pulse ( $-120$  to  $-50$  mV) for 9 s. The channels that remain available after each inactivating pulse were assessed by the peak currents during the following short test pulse to 0 mV for 10 ms. The fraction available is defined as the normalized peak current (relative to the current evoked with an inactivating pulse at  $-120$  mV) and is plotted against the voltage of the inactivating pulse. Two sets of control data were obtained before and after the experiments in different concentrations of imipramine to demonstrate the absence of significant voltage drift during this long experiment. The lines are fits to each set of data of a Boltzmann function: fraction available =  $1/(1 + \exp[(V - V_h)/k])$ , with  $V_h$  values (in mV) of  $-71.8$ ,  $-72.8$ ,  $-74.9$ ,  $-76.8$ ,  $-84.0$ , and  $-91.2$ ; and  $k$  values of 5.4, 5.5, 5.9, 5.9, 5.9, and 6.3 for control (before imipramine), control (after imipramine), 1, 3, 10, and 30  $\mu\text{M}$  imipramine; respectively. B, shift of the inactivation curve ( $\Delta V$ ) is determined in each cell by the difference between  $V_h$  in control and in the presence imipramine, and are  $3.4 \pm 0.3$ ,  $5.6 \pm 0.9$ ,  $6.6 \pm 0.4$ , and  $25.9 \pm 1.1$  (mV,  $n = 3$  to 4) for 1, 3, 10, and 30  $\mu\text{M}$  imipramine, respectively. C,  $\Delta V/k$  values are calculated for each drug concentration in each cell. The mean value of  $\Delta V/k$  in each drug concentration ( $n = 3$  to 4) is used to calculate  $\exp(\Delta V/k)$ , which is plotted against imipramine concentration. The line is a fit to the data of the form:  $\exp(\Delta V/k) = [1 + (D/1.2)]/[1 + (D/1000)]$ , where  $D$  denotes imipramine concentration in micromolar (see text for more details).

with a  $K_{app}$  defined by (Bean, 1984; Kuo and Bean, 1994):  $K_{app} = 1/[h/K_R + (1 - h)/K_I]$ , where  $h$  is the fraction of channels in state R in the absence of drug ("fraction available" in the control condition of Fig. 3A), and  $K_R$  and  $K_I$  are the dissociation constants for the resting and inactivated channels, respectively. This is as if the overall affinity of imipramine to the channel ( $\sim 1/K_{app}$ ) is a weighted average of the affinity toward each state of the channel  $[h/K_R + (1 - h)/K_I]$ . According to this equation and a  $K_{app}$  of  $\sim 1.4 \mu\text{M}$  at  $-50 \text{ mV}$ , where  $h$  is  $\sim 0.05$  (Fig. 3A),  $K_I$  should be  $\sim 1.3 \mu\text{M}$ . With a  $K_I$  of  $\sim 1.3 \mu\text{M}$  and a  $K_{app}$  of  $\sim 130 \mu\text{M}$  at  $-120 \text{ mV}$  where  $h$  is close to 1 (Fig. 3A),  $K_R$  must be somewhat larger than  $130 \mu\text{M}$ . In other words,  $K_I$  and  $K_R$  must differ by at least 100-fold.

**Measurement of the Affinity between Inactivated  $\text{Na}^+$  Channels and Imipramine by Shift of the Inactivation Curve.** One may also estimate  $K_I$  with another approach based on the foregoing scheme. In the control condition, the inactivation curve can be approximated by a Boltzmann distribution,  $1/(1 + \exp[(V - V_h)/k])$  (Fig. 3A), where  $V$  is the membrane potential,  $V_h$  is the half-inactivated potential (at which half of the channels are in state R and the other half are in state I), and  $k$  is the slope factor. When imipramine is added, the shape of the curve should remain the same, but the midpoint ( $V_h$ ) would be shifted by  $\Delta V$ , which is related to  $K_I$  and  $K_R$  by equating  $\exp(\Delta V/k)$  with  $[1 + (D/K_I)]/[1 + (D/K_R)]$ , where  $D$  is the concentration of imipramine (Bean et al., 1983; Bean, 1984). Figure 3, A and B, show that with 1 to  $30 \mu\text{M}$  imipramine added, the inactivation curves indeed are shifted leftward with unchanged slope. Figure 3C shows the mean  $\exp(\Delta V/k)$  values in various concentrations of imipramine and a fit with the foregoing equation, revealing a  $K_I$  of  $1.2 \mu\text{M}$  if  $K_R$  is assumed to be  $1000 \mu\text{M}$ . If  $K_R$  is assumed to be 100 and  $10,000 \mu\text{M}$ ,  $K_I$  would be 1 and  $1.2 \mu\text{M}$ , respectively. This is quite consistent with the  $K_I$  value ( $\sim 1.3 \mu\text{M}$ ) obtained from a totally different approach in Fig. 2.

**Binding Rate of Imipramine onto the Inactivated  $\text{Na}^+$  Channel.** We also explored the kinetics of interaction between imipramine and the inactivated  $\text{Na}^+$  channels. Figure 4 shows that after a few milliseconds at a recovery gap potential, the majority of normal inactivated channels recover, whereas most imipramine-bound channels do not. Because imipramine-bound inactivated channels recover much more slowly than "normal" inactivated channels, one may assess the binding rate of imipramine onto inactivated  $\text{Na}^+$  channels by another voltage protocol, in which the prepulse is gradually lengthened while the  $-120 \text{ mV}$  gap is fixed at 5 ms (Fig. 5A). The decrease of  $\text{Na}^+$  currents elicited during the test pulse subsequent to the  $-120 \text{ mV}$  gap now mostly reflects the increase of drug-bound inactivated channels, with a little contamination from the concomitant increase of normal inactivated channels that have not recovered during the 5-ms gap. The contamination is corrected by taking the difference between the  $\text{Na}^+$  current in control and that in the presence of imipramine (Fig. 5B). Figure 5C shows that the macroscopic binding rates increase linearly with drug concentration, supporting the presumption in Fig. 2 that low concentrations of imipramine interacts with  $\text{Na}^+$  channels via a one-to-one binding process (simple bimolecular reaction). The linear regression fit to the data reveals a binding rate constant of  $1.5 \times 10^5 \text{ M}^{-1}\text{s}^{-1}$ .

**Imipramine Inhibition of Inactivation-Deficient Mutant RIIA  $\text{Na}^+$  Channels.** We have seen that imipramine has much higher affinity for inactivated channels than the resting channels. Considering that resting  $\text{Na}^+$  channels are quickly activated and then inactivated upon membrane depolarization, could the drug receptor be formed during channel activation? To test for this possibility, we examined the effect of imipramine on inactivation-deficient (F1489Q) mutant RIIA  $\text{Na}^+$  channels. Figure 6A shows that in the control condition, the F1489Q mutant  $\text{Na}^+$  current initially decays quickly (but only to a very small extent) and then quickly enters another very slow decay phase. The two phases of current decay presumably are ascribable to the residual fast inactivation process and the slow inactivation process (which is probably like the C-type inactivation in  $\text{K}^+$  channels; Lawrence et al., 1996; Nuss et al., 1996), respectively. Imipramine (10 to  $100 \mu\text{M}$ ) apparently inhibits the mutant  $\text{Na}^+$  current by dose-dependent acceleration of current decay. For simplicity, we did not fit multiexponential function to describe the kinetics of current decay. Instead, we left out the first 9 ms and fit monoexponential function to the rest part of

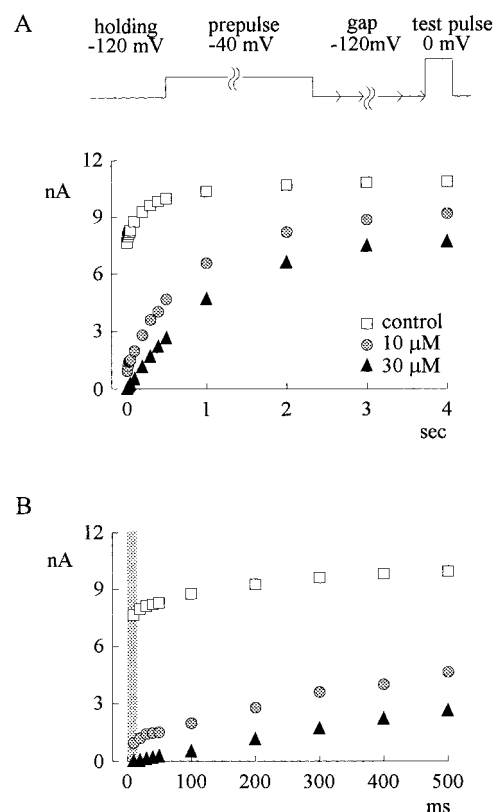


**Fig. 4.** Unbinding rate of imipramine from  $\text{Na}^+$  channels. A, in control or in the continuous presence of 10 to  $30 \mu\text{M}$  imipramine, the cell was held at  $-120 \text{ mV}$  and then prepulsed to  $-40 \text{ mV}$  for 8 s. The cell was then stepped back to a recovery gap potential at  $-120 \text{ mV}$  for variable length before being stepped again to a short test pulse at  $0 \text{ mV}$  for 6 ms to assess the available current. The pulse protocol was repeated every 15 s. The time courses of recovery are obtained by plotting the peak current at the test pulse against the length of the recovery gap potential. With very long ( $\sim 4 \text{ s}$ ) recovery gap potential, the currents in 10 to  $30 \mu\text{M}$  imipramine recover to their steady-state block level at  $-120 \text{ mV}$ , and thus are still smaller than the current at that time point in control. B, data in the first 500 ms of recovery gap are redrawn with a smaller horizontal scale to demonstrate that after short (e.g., 5–10 ms) recovery period, the currents in control have largely recovered, but most currents in imipramine have not.

the currents. Omission of the fast transient component of the current may underestimate the kinetics of imipramine binding, but this approach gives reasonable fits to the current and should be valid enough for further discussion (see below). Figure 6B plots the rate of the current decay against imipramine concentration (0 to 100  $\mu\text{M}$ ), and reveals a binding rate constant of  $2.3$  to  $4.0 \times 10^5 \text{ M}^{-1}\text{s}^{-1}$ . Based on the hinged-lid model of Na<sup>+</sup> channel inactivation, F1489Q mutation presumably weakens binding of the inactivating "lid"

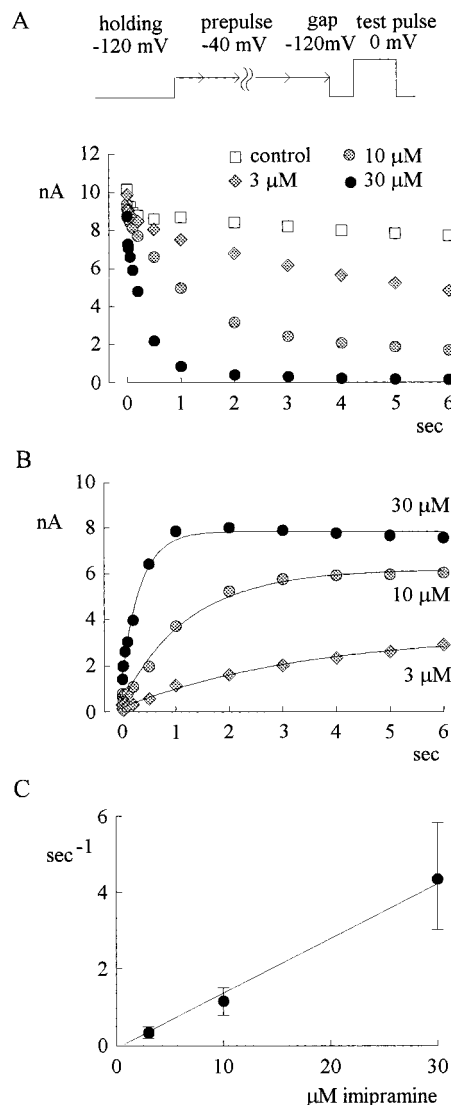


**Fig. 5.** Binding rate of imipramine onto the inactivated Na<sup>+</sup> channel. A, in control, 3, 10, and 30  $\mu\text{M}$  imipramine, the cell was held at  $-120 \text{ mV}$  and prepulsed to  $-40 \text{ mV}$  for variable length. Immediately after the prepulse, there is a recovery gap potential at  $-120 \text{ mV}$  for 5 ms to recover normal (not imipramine-bound) inactivated Na<sup>+</sup> channels, and then the available channels are assessed by a short test pulse to  $0 \text{ mV}$  for 10 ms. The pulse protocol is repeated every 15 s. The peak Na<sup>+</sup> current at the test pulse is plotted against the duration of the prepulse to demonstrate the decay of the peak currents as the prepulse lengthens. B, the difference between the current in imipramine and the current in control (data from part A) is plotted against the duration of the prepulse. The lines are monoexponential fits of the form: current (nA) =  $3.38 - 3.19 \times \text{Exp}(-t/3.37)$  ( $t$  denotes length of prepulse in seconds, the horizontal axis), current =  $6.19 - 5.72 \times \text{Exp}(-t/1.26)$ , and current =  $7.86 - 6.25 \times \text{Exp}(-t/0.35)$  for 3, 10, and 30  $\mu\text{M}$  imipramine, respectively. C, the inverses of the time constants in part B ( $n = 3$  to 5) are plotted against the concentration of imipramine. The line is a linear regression fit to the mean values. The intercept and slope are  $0.14 \text{ s}^{-1}$  and  $1.5 \times 10^5 \text{ M}^{-1}\text{s}^{-1}$ , respectively.

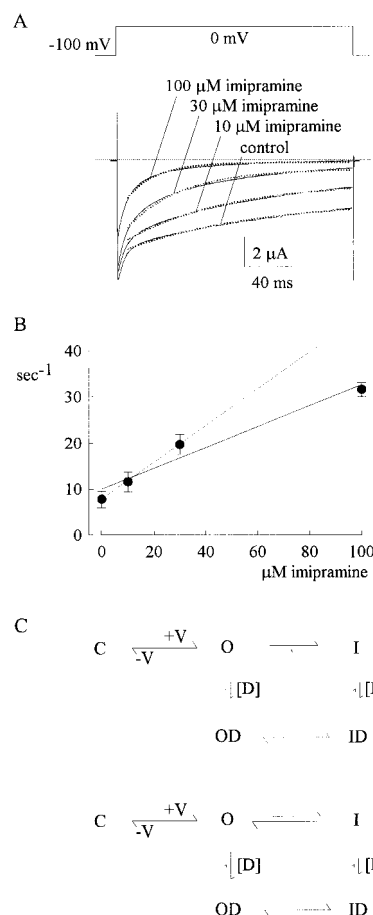


**Fig. 6.** Inhibition of the inactivation-deficient F1489Q Na<sup>+</sup> channel by imipramine. A, the oocyte was held at  $-100 \text{ mV}$  and stepped to  $0 \text{ mV}$  for 200 ms every 10 s. Decay of the current has a rapid initial phase and a subsequent slow phase, and 10 to 100  $\mu\text{M}$  imipramine obviously accelerates both phases in a dose-dependent fashion. To simplify the analysis, we try to describe only the more sustained component (9th to 200th ms) of the currents with monoexponential functions (the thick dotted lines), which seem to give reasonable fits to this part of the data. The thin dotted line indicates the zero current level. B, the mean value of the inverses of time constants from the fits in part A ( $n = 3$  to 5) are plotted against the concentration of imipramine. The solid line is a linear regression fit to the data in 0 to 100  $\mu\text{M}$  imipramine. The intercept and slope are  $9.7 \text{ s}^{-1}$  and  $2.3 \times 10^5 \text{ M}^{-1}\text{s}^{-1}$ , respectively. This fit, however, does not seem to be optimal. It may be better to describe the first three data points in 0 to 30  $\mu\text{M}$  imipramine by another linear regression (the dotted line, slope  $4.0 \times 10^5 \text{ M}^{-1}\text{s}^{-1}$ ), with the point in 100  $\mu\text{M}$  imipramine falling below the trend formed by the first three points. This is reminiscent of the case of imipramine block of open A type K<sup>+</sup> channels (Kuo, 1998b), suggesting that the macroscopic binding rate of 100  $\mu\text{M}$  imipramine to the open Na<sup>+</sup> channel is no longer much slower than the channel activation rate in the oocyte preparation, and thus may serve as a collateral evidence arguing for open Na<sup>+</sup> channel block by imipramine. C, two simplified gating schemes for the discussion of imipramine action on the wild-type (top) and mutant Na<sup>+</sup> channels (bottom). C, O, I, OD, and ID stand for the closed (resting or deactivated), open (activated), inactivated, open-imipramine bound, and inactivated-imipramine bound states, respectively.  $+V$  (depolarization) and  $-V$  (hyperpolarization) facilitate channel activation and deactivation, respectively. In the wild-type channels the O-to-I rate is very fast, yet the I-to-O rate is much slower, making steady-state distribution of the channel mostly in the inactivated state. Imipramine binds to the inactivated state with a binding rate linearly correlated with the drug concentration (ID) and a slow unbinding rate. The binding of imipramine to the open wild-type channels is uncertain at this point (the dotted arrows between state O and OD in the upper). In the mutant channels the I-to-O rate presumably increases a lot, resulting in the aforementioned two phases of current decay. Because the data from mutant channel indicate substantial and even faster binding rate to the open channels of imipramine than to the inactivated channels, the arrows between states O and OD in the lower are drawn with solid lines, and the arrow from O to OD is made larger than that from I to ID (see text for more detail).



to the channel pore, leading to a much faster transition rate from state I to state O in the mutant than in the wild-type channels (Fig. 6C). Under such circumstances, even if imipramine did not bind to and block open  $\text{Na}^+$  channel, it could still accelerate current decay by stabilizing channels in the ID state and thus effectively decreasing chances (speed) of the I-to-O transition. However, we have noted that in the mutant channel the I-to-O rate is much faster than O-to-I rate, which is already  $\sim 1500 \text{ s}^{-1}$  (the inverse of the time constant of macroscopic current decay in wild-type channels). The very fast O-to-I and I-to-O rates thus should make a rapid "equilibrium" of the channel protein between states O and I from the viewpoint of the relatively much slower imipramine binding process. Because this rapid "equilibrium" between states O and I very much favors state O, the apparent imipramine binding rate here should be much slower than the I to ID rate documented in Fig. 5 if imipramine could only bind to the inactivated state. This is inconsistent with the experimental finding of  $2.3$  to  $4.0 \times 10^5 \text{ M}^{-1}\text{s}^{-1}$ , which is probably an underestimate, because we have left out the rapid initial rapid decay phase in fitting, yet it is already faster or at least not much slower than the binding rate to the inactivated state ( $1.5 \times 10^5 \text{ M}^{-1}\text{s}^{-1}$ , Fig. 5). Imipramine thus is unlikely to speed the decay of macroscopic  $\text{Na}^+$  currents by selective binding to only the inactivated channels. Instead, imipramine seems to bind to the open channel and block the pore, most likely with an even faster binding rate than that to the inactivated channels. The fact that imipramine significantly binds to and blocks the mutant channel would also suggest that formation of the imipramine binding site is not directly related to binding of the inactivating hinged-lid to the  $\text{Na}^+$  channel pore (Vedantham and Cannon, 1999).

**Imipramine Binding to Open  $\text{Na}^+$  Channels with Very Fast Kinetics.** In Fig. 2, we have noted that in addition to selective binding to and thus stabilizing the inactivated  $\text{Na}^+$  channels, there is another inhibitory effect that becomes manifest with high concentrations ( $> 30 \mu\text{M}$ ) of imipramine. In view of the findings in Fig. 6, the additional inhibitory effect of high concentrations of imipramine in Fig. 2 might be related to open channel block. This blocking effect may significantly affect the amplitude and kinetics of the macroscopic current only when the concentration of imipramine is high enough, because the very rapid and complete inactivation in native  $\text{Na}^+$  channels would require a fast macroscopic binding (and thus blocking) rate of imipramine to produce discernible changes in the  $\text{Na}^+$  current (see below). To explore such a possibility, we carefully examined the kinetics of  $\text{Na}^+$  current decay in the presence of imipramine. The gradual decrease of peak  $\text{Na}^+$  currents in Fig. 7A demonstrates use-dependent block, indicating gradual increase of unavailable channels (gradual stabilization of the  $\text{Na}^+$  channels to the inactivated state) by  $100 \mu\text{M}$  imipramine in the first few pulses repeated at a frequency of  $1 \text{ Hz}$ . In contrast to the gradual change of the peak current, the kinetics of the current decay changes abruptly. As soon as the cell is moved from the control solution into the external solution containing  $100 \mu\text{M}$  imipramine, the kinetics of the macroscopic current decay are immediately accelerated to the same extent in all sweeps (Fig. 7B). There is also a tendency for the current peak to appear earlier in imipramine. Figure 7C further shows that the acceleration of current decay (the difference between the rates of macroscopic current decay in control and

in the presence of imipramine) is linearly correlated with imipramine concentration, giving a macroscopic binding rate constant of  $1.1 \times 10^7 \text{ M}^{-1}\text{s}^{-1}$ . This value is apparently faster than that from the mutant channels expressed in oocytes ( $2.4$  to  $4.0 \times 10^5 \text{ M}^{-1}\text{s}^{-1}$ ), chiefly because the latter is probably an underestimate. Because the  $\text{Na}^+$  channel in native hippocampal neurons shows rapid and almost complete inactivation, the I-to-O rate should be very much slower than the O-to-I rate (which is essentially the absolute determinant of the decaying speed of the macroscopic currents; Fig. 6C, top). It is unlikely that further decrease of the already very slow I-to-O rate by absorption of channels to state ID would make the dose-dependent acceleration of current decay by imipra-

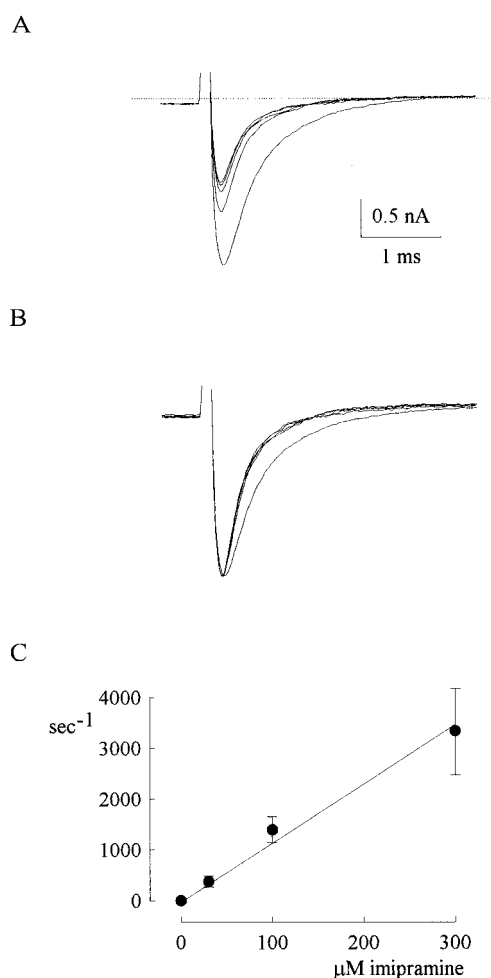


**Fig. 7.** Binding rate of imipramine onto the open  $\text{Na}^+$  channel. A,  $\text{Na}^+$  currents in control or  $100 \mu\text{M}$  imipramine were recorded in a neuron. The cell was held at  $-120 \text{ mV}$  and stepped to  $+10 \text{ mV}$  for  $7 \text{ ms}$  every second. After the change of external solution from control to  $100 \mu\text{M}$  imipramine, peak of the  $\text{Na}^+$  current gradually decreases within a few sweeps to reach a steady-state level. B, the  $\text{Na}^+$  currents in  $100 \mu\text{M}$  imipramine in part A are scaled up so that every current sweep has the same peak as that of the control current. It is evident that the kinetics of current decay does not change gradually, but is accelerated to the same extent in all sweeps in  $100 \mu\text{M}$  imipramine. Also note that the current peak tends to appear slightly earlier in imipramine. C, decay of the macroscopic  $\text{Na}^+$  currents in control and in  $30$  to  $300 \mu\text{M}$  imipramine is fitted with monoexponential functions. In each cell, the inverse of the time constant in control is subtracted from the inverse of the time constant in the presence of drug to give the macroscopic binding rate of imipramine to the open  $\text{Na}^+$  channels ( $n = 3$  to  $6$ ). The macroscopic binding rate is then plotted against the concentration of imipramine. The line is the linear regression fit with a slope of  $1.1 \times 10^7 \text{ M}^{-1}\text{s}^{-1}$ .

mine in Fig. 7. Thus the linear correlation between the acceleration of decaying kinetics and imipramine concentration, along with the slightly earlier peak in imipramine than in control, would strongly argue that imipramine blocks the open Na<sup>+</sup> channel pore with a one-to-one binding process, exactly analogous to imipramine binding to the inactivated channels. However, in native hippocampal neurons, imipramine binding to the open Na<sup>+</sup> channel (Fig. 7C) is evidently ~70-fold faster than its binding to the inactivated channel (Fig. 5C).

**Block of Open Na<sup>+</sup> Channels by Carbamazepine and Diphenhydramine.** Similar to imipramine, high concentrations of carbamazepine and diphenhydramine also accelerate the kinetics of macroscopic Na<sup>+</sup> current decay (Fig. 8, A and B). Figure 8C further shows that the acceleration of macroscopic current decay is linearly correlated with carbamazepine and diphenhydramine concentration, giving binding rate constants of  $1.1 \times 10^6$  and  $8.3 \times 10^5$  M<sup>-1</sup>s<sup>-1</sup> for carbamazepine and diphenhydramine, respectively. These rates are again significantly faster than the previously reported binding rates of carbamazepine and diphenhydramine onto the inactivated Na<sup>+</sup> channels (Kuo et al., 1997, 2000). In contrast, the kinetics of current decay are not definitely accelerated in 100 to 300 μM lamotrigine. Because the Na<sup>+</sup> current generally decays with a speed of ~1500 s<sup>-1</sup> due to fast inactivation, the macroscopic binding rate of a pore-blocking drug probably should be at least 150 s<sup>-1</sup> (a binding rate constant of  $5 \times 10^5$  M<sup>-1</sup>s<sup>-1</sup> for 300 μM drug) to make discernible acceleration of the current decay on top of the fast inactivation. The binding rate constant of lamotrigine onto the inactivated Na<sup>+</sup> channel is only ~10,000 M<sup>-1</sup>s<sup>-1</sup> (Kuo and Lu, 1997). It seems that binding of lamotrigine onto the open Na<sup>+</sup> channel is not as fast as  $5 \times 10^5$  M<sup>-1</sup>s<sup>-1</sup> (~50 times faster than its binding onto the inactivated channel); consequently, no definite changes in the kinetics of the Na<sup>+</sup> current decay in 100 to 300 μM lamotrigine.

## Discussion

**Imipramine As an Inactivation Stabilizer: The Accessory Role of the Tertiary Amine Chain.** In this study, we demonstrate that imipramine binds to the inactivated neuronal Na<sup>+</sup> channels with a dissociation constant of ~1.3 μM, whereas the affinity between imipramine and the resting channels is at least 100 times lower (Figs. 2 and 3). Imipramine is thus similar to anticonvulsants phenytoin, carbamazepine, and lamotrigine in selective binding to the inactivated channels (Kuo and Bean, 1994; Kuo et al., 1997; Kuo and Lu, 1997). Given a one-to-one binding process, a binding rate of  $1.5 \times 10^5$  M<sup>-1</sup>s<sup>-1</sup> (Fig. 5), and a dissociation constant of 1.3 μM, imipramine should unbind from the inactivated Na<sup>+</sup> channels at a rate of ~0.19 s<sup>-1</sup>. In the same preparation, the unbinding rate of carbamazepine is ~0.95 s<sup>-1</sup> (calculated from a binding rate of  $\sim 3.8 \times 10^4$  M<sup>-1</sup>s<sup>-1</sup> and a dissociation constant of ~25 μM to the inactivated Na<sup>+</sup> channels; Kuo et al., 1997). The ~20-fold difference in overall binding affinity indicates a difference of ~3 RT (~1.8 kcal/mol; R is the gas constant and T is the absolute temperature) in the total binding energy between the two drugs. Because imipramine and carbamazepine share the same three-dimensional structure in the diphenyl motif (Fig. 1A), the tertiary amine chain present in imipramine but not in carbamazepine

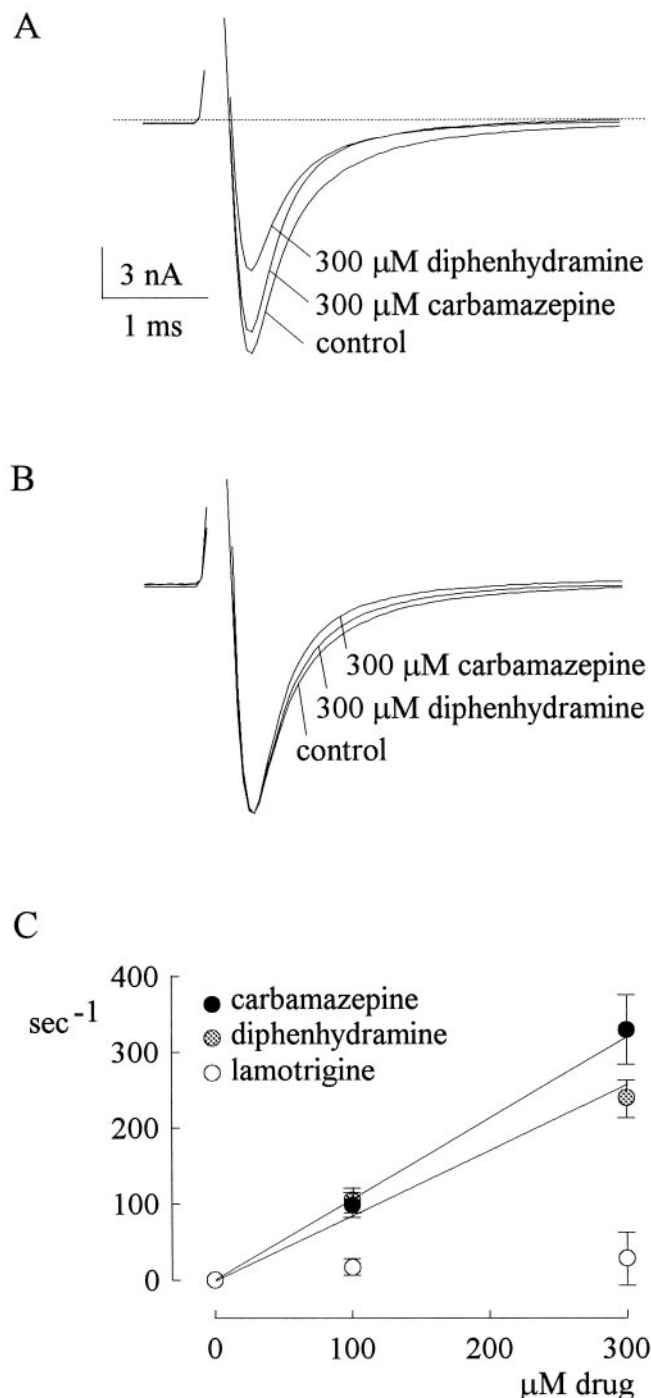


**Fig. 8.** Binding rates of carbamazepine and diphenhydramine onto the open Na<sup>+</sup> channel. A, Na<sup>+</sup> currents in control, 300 μM carbamazepine, and 300 μM diphenhydramine were recorded in the same neuron. The pulse protocol is the same as that in Fig. 7A. B, the same currents in part A are scaled to the same peak amplitude to demonstrate acceleration of current decay by carbamazepine and diphenhydramine. C, for 100 to 300 μM carbamazepine, diphenhydramine, and lamotrigine, the macroscopic binding rate is obtained by the same approach as that described in Fig. 7C, and then is plotted against the drug concentration ( $n = 4$  to 9). The lines are linear regression fits with slopes of  $1.1 \times 10^6$  M<sup>-1</sup>s<sup>-1</sup> and  $8.3 \times 10^5$  M<sup>-1</sup>s<sup>-1</sup> for carbamazepine and diphenhydramine, respectively. The macroscopic binding rate of 100 to 300 μM lamotrigine is not significantly different from the zero point, indicating insignificant change of the decaying kinetics of Na<sup>+</sup> current in the presence of 100 to 300 μM lamotrigine.



probably is responsible for the  $\sim 3$  RT difference in binding energy. If one assumes negligible contribution to the binding energy by the short amide group in carbamazepine and a total binding energy of 13.6 RT (dissociation constant,  $\sim 1.3 \mu\text{M}$ ) for imipramine binding to the inactivated  $\text{Na}^+$  channel, then probably  $\sim 22\%$  ( $3/13.6$ ) of the total binding energy of imipramine is contributed by the tertiary amine chain, and the major part ( $\sim 78\%$ ) of binding energy is from the diphenyl motif. Because 1.8 kcal/mol is much smaller than the usual strength of ionic bonds (5 to 10 kcal/mol), this tertiary amine chain probably interacts with the channel protein by the other binding forces such as hydrogen bond, ion-dipole, or hydrophobic interactions (Zimmerman and Feldman, 1989). This is consistent with the findings that the potency of *n*-alkanols in blocking  $\text{Na}^+$  channels is related to not only phenyl substitution, but also intrinsic molar volume, hydrogen bond acceptor basicity as well as donor acidity, and the polarity of the alkanols (Kondratiev and Hahin, 2001). According to the foregoing kinetic analysis, the overall  $\sim 20$ -fold difference in the binding affinity between imipramine and carbamazepine can be divided into a 5-fold difference in the unbinding rate and a 4-fold difference in the binding rate. The tertiary amine chain thus seems to increase the probability of effective collision (between the free drug molecule and the vacant receptor) and the binding strength (between the bound drug molecule and the occupied receptor) of imipramine roughly equally.

**Imipramine As an Open Channel Blocker: Blocking the External Pore Mouth by the Diphenyl Motif.** In addition to stabilizing inactivation, imipramine also inhibits the inactivation-deficient mutant  $\text{Na}^+$  channels expressed in oocytes (Fig. 6). This is consistent with previous findings that phenytoin would inhibit  $\text{Na}^+$  currents when fast inactivation was removed by enzymes (Schauf et al., 1976; Quandt, 1988). In Figs. 7 and 8, we further demonstrate dose-dependent acceleration of current decay by imipramine, carbamazepine, and diphenhydramine in native channels, indicating the role of these drugs as open  $\text{Na}^+$  channel blockers and the location of the drug receptor in or near the pore. Because carbamazepine could also block the open  $\text{Na}^+$  channel, imipramine probably blocks ion conduction chiefly with the diphenyl motif rather than the tertiary amine chain. In this regard, it is interesting to note that phenytoin, carbamazepine, and lamotrigine probably bind to the same anticonvulsant receptor on the external side of the channel with the common diphenyl structural motif (Kuo, 1998a), although an internally located local anesthetic receptor that overlaps with the anticonvulsant receptor has also been proposed (see Ragsdale et al., 1994, 1996; Yarov-Yarovoy et al., 2001; but also see Li et al., 1999). Finally, because of its size ( $\sim 10 \text{ \AA}$  in diameter), imipramine is unlikely to plug deeply into the pore. These arguments altogether might locate the anticonvulsant receptor to the relatively wide external pore mouth of the  $\text{Na}^+$  channel, with pore-blocking effect produced chiefly by binding of the phenyl groups of the drugs. Gating conformational changes involving this area and causing different drug affinity are plausible, as it has been shown that externally located mutations or conformational changes could have an effect on  $\text{Na}^+$  channel inactivation (Chahine et al., 1994; Yang and Horn, 1995; Ji et al., 1996), and a mutation in the external pore loop may alter  $\text{Na}^+$  channel activation and deactivation (Tomaselli et al., 1995). Also, imipramine is an external open

channel blocker but not an inactivation stabilizer in A-type  $\text{K}^+$  channels (Kuo, 1998b). This could suggest subtle yet significant difference in the gating conformational changes in the external pore mouth of  $\text{K}^+$  and  $\text{Na}^+$  channels.

**Continual Gating Conformational Changes in the Anticonvulsant Receptor.** Upon depolarization,  $\text{Na}^+$  channels undergo a series of conformational changes leading to channel opening (activation) and inactivation. Although not necessarily so, inactivation tends to happen after activation (and thus we have the simplified C-O-I scheme in Fig. 6C). If imipramine and carbamazepine are open channel blockers, the anticonvulsant receptor should be formed during channel activation (the C-to-O step in Fig. 6C). Because the channel cannot be simultaneously occupied by two anticonvulsant molecules (Kuo, 1998a), presumably there is only one anticonvulsant receptor in the channel. Thus there should be additional conformational changes affecting either the receptor or the access to the receptor during inactivation to account for the  $\sim 70$ -fold slower binding rates of imipramine to the inactivated than to the open  $\text{Na}^+$  channels (Figs. 5 and 7; for simplicity, we will assume changes in the receptor in the following discussion, but similar or slightly modified arguments may apply to changes in the access to the receptor). The slow drug binding rate to the inactivated  $\text{Na}^+$  channel, one of the key attributes leading to the "use-dependent" block of  $\text{Na}^+$  current, thus is not a fixed feature but is achieved by further modification of a well-developed receptor. In comparison with the  $\sim 70$ -fold difference between the binding rates onto the open and the inactivated channels for imipramine (Figs. 5 and 7), the difference is  $\sim 30$ -fold for carbamazepine ( $1.1 \times 10^6$  versus  $4 \times 10^4 \text{ M}^{-1}\text{s}^{-1}$ , Fig. 8; Kuo et al., 1997), yet is only  $\sim 10$ -fold for diphenhydramine ( $8.2 \times 10^5$  versus  $7.2 \times 10^4 \text{ M}^{-1}\text{s}^{-1}$ , Fig. 8; Kuo et al., 2000). The difference thus is more similar between carbamazepine and imipramine than between diphenhydramine and imipramine, suggesting that the conformational changes in the receptor site during channel inactivation probably involve the binding ligands for the diphenyl motif more than those for the amine chain. Along with the stronger inhibitory effect of the drugs with tertiary amine chain (than the drugs with only the diphenyl motif) on resting channels (Kuo et al., 2000), it seems plausible that the binding ligands for the amine chain do not have conformational changes as dramatic as the ligands for the diphenyl motif during the whole gating process of the channel. The structure of the diphenyl motif in diphenhydramine is different from that in imipramine and carbamazepine chiefly in the torsion angles ( $\sim -60^\circ$  and  $\sim -70^\circ$  versus  $\sim -60^\circ$  and  $\sim +50$  to  $+60^\circ$ , Kuo et al., 2000). It is surprising that the torsion angle, which is usually a quite freely movable parameter, should have such a significant effect on drug-binding kinetics. This would suggest delicate geometric requirement of the binding counterparts for effective collision. If the binding ligands of the planar phenyl groups are also planar phenyl groups (to allow close proximity between the binding counterparts), then the torsion angles of the binding ligands in the receptor (presumably aromatic side chains of the amino acids in the channel peptide) are probably more "fixed" than those in single free-moving amino acids. During  $\text{Na}^+$  channel activation, these aromatic ligands are oriented to make an effective binding site for the diphenyl motif in the dibenzazepine tricyclic structure of carbamazepine and imipramine and are further reoriented

by subsequent gating conformational changes that lead to inactivation. The diphenyl motif seems to change chiefly in the torsion angles during this reorientation and becomes quite less favorable for the binding of imipramine and carbamazepine (but not so much for the binding of diphenhydramine whose two aromatic groups are oriented differently from those in the dibenzazepine tricyclic structure).

**Pharmacological and Therapeutic Implications.** The therapeutic plasma concentrations of imipramine and diphenhydramine is usually 0.1 to 1  $\mu$ M. However, the free drug concentration in the cerebrospinal fluid probably is no more than  $\sim$ 0.1  $\mu$ M because of  $\sim$ 90% plasma protein binding of the drugs (Carruthers et al., 1978; Amsterdam et al., 1980; Benet et al., 1996). This concentration is too low to have a significant effect on the Na<sup>+</sup> channels according to the data from this study. On the other hand, we have argued that carbamazepine could be more effective in suppressing short ictal depolarization than phenytoin because of its faster binding rate to the inactivated Na<sup>+</sup> channels (Kuo et al., 1997). With the even faster  $\sim$ 30-fold binding rate to the open Na<sup>+</sup> channel, carbamazepine may have an overall use-dependent inhibitory effect on the cellular discharges happening even faster than we previously imagined. This would be especially true in the cases whose ictal activities are characterized by only periodic bursts of discharges but not vivid sustained depolarization to keep the Na<sup>+</sup> channels in the inactivated state, such as typical absence seizures. Although carbamazepine is not a drug of choice, in quite a few earlier reports some patients with absence seizures do respond satisfactorily to carbamazepine (Schain et al., 1977; Familusi, 1985). Such a therapeutic effect is difficult to envisage if one considers only binding to the inactivated channels. It is plausible that binding to and blocking the open neuronal Na<sup>+</sup> channel may play a role in the clinical effect of carbamazepine.

## References

- Amsterdam J, Brunswick D, and Mendels J (1980) The clinical application of tricyclic antidepressant pharmacokinetics and plasma levels. *Am J Psychiatry* **137**:653–663.
- Balser JR, Nuss HB, Orias DW, Jones DC, Marban E, Tomaselli GF, and Lawrence JH (1996) Local anesthetics as effectors of allosteric gating: lidocaine effects on inactivation-deficient rat skeletal muscle Na channels. *J Clin Invest* **98**:2874–2886.
- Bean BP (1984) Nitrendipine block of cardiac calcium channels: high-affinity binding to the inactivated state. *Proc Natl Acad Sci USA* **81**:6386–6392.
- Bean BP, Cohen CJ, and Tsien RW (1983) Lidocaine block of cardiac sodium channels. *J Gen Physiol* **81**:613–642.
- Benet LZ, Fie S, and Schwartz JB (1996) Design and optimization of dosage regimens: pharmacokinetic data, in *Goodman and Gilman's The Pharmacological Basis of Therapeutics*, 9th ed (Hardman JG, Limbird LE, Molinoff PB, and Ruddon RW eds) pp. 1707–1711, 1749, McGraw-Hill, New York.
- Bennett PB, Valenzuela C, Chen L-Q, and Kallen RG (1995) On the molecular nature of the lidocaine receptor of cardiac Na<sup>+</sup> channels: modification of block by alterations in the  $\alpha$ -subunit III-IV interdomain. *Circ Res* **77**:584–592.
- Benz I and Kohlhardt M (1992) Differential response of DPI-modified cardiac Na<sup>+</sup> channels to antiarrhythmic drugs: no flicker blockade by lidocaine. *J Membr Biol* **126**:257–263.
- Bolotina V, Courtney KR, and Khodorov B (1992) Gate-dependent blockade of sodium channels by phenothiazine derivatives: structure-activity relationships. *Mol Pharmacol* **42**:423–431.
- Butterworth JF and Strichartz GR (1990) Molecular mechanisms of local anesthesia: a review. *Anesthesiology* **72**:711–734.
- Carruthers SG, Shoeman DW, Hignite CE, and Azarnoff DL (1978) Correlation between plasma diphenhydramine level and sedative and antihistamine effects. *Clin Pharmacol Ther* **23**:375–382.
- Chahine M, George AL, Zhou M, Ji S, Sun W, Barchi R, and Horn R (1994) Sodium channel mutations in paramyotonia congenita uncouple inactivation from activation. *Neuron* **12**:281–294.
- Clarkson CW, Follmer CH, Ten Eick RE, Hondeghem LM, and Yeh JZ (1988) Evidence for two components of sodium channel block by lidocaine in isolated cardiac myocytes. *Cir Res* **63**:869–878.
- Familusi JB (1985) Preliminary Nigerian experience in the use of carbamazepine in children with intractable seizures. *Epilepsia* **26**:10–14.
- Ji S, George AL, Horn R, and Barchi RL (1996) Paramyotonia congenita mutations reveal different roles for segments S3 and S4 of domain D4 in hSkM1 sodium channel gating. *J Gen Physiol* **107**:183–194.
- Kondratiev A and Hahn R (2001) ED50 GNa block predictions for phenyl substituted and unsubstituted n-alkanols. *J Membr Biol* **180**:123–136.
- Kuo C-C (1998a) A common anticonvulsant binding site for phenytoin, carbamazepine and lamotrigine in neuronal Na<sup>+</sup> channels. *Mol Pharmacol* **54**:712–721.
- Kuo C-C (1998b) Imipramine inhibition of transient K<sup>+</sup> current: An external open channel blocker preventing fast inactivation. *Biophys J* **75**:2845–2857.
- Kuo C-C and Bean BP (1994) Slow binding of phenytoin to inactivated sodium channels in rat hippocampal neurons. *Mol Pharmacol* **46**:716–725.
- Kuo C-C, Chen R-S, Lu L, and Chen RC (1997) Carbamazepine inhibition of neuronal Na<sup>+</sup> currents: quantitative distinction from phenytoin and possible therapeutic implications. *Mol Pharmacol* **51**:1077–1083.
- Kuo C-C, Huang R-C, and Lou B-S (2000) Inhibition of Na<sup>+</sup> current by diphenhydramine and other diphenyl compounds: molecular determinants of selective binding to the inactivated channels. *Mol Pharmacol* **57**:135–143.
- Kuo C-C and Lu L (1997) Characterization of lamotrigine inhibition of Na<sup>+</sup> channels in rat hippocampal neurons. *Br J Pharmacol* **121**:1231–1238.
- Lawrence JH, Orias DW, Balser JR, Nuss HB, Tomaselli GF, O'Rourke B, and Marban E (1996) Single-channel analysis of inactivation-defective rat skeletal muscle sodium channel containing the F1304Q mutation. *Biophys J* **71**:1285–1294.
- Li H-L, Galue A, Meadows L, and Ragsdale DS (1999) A molecular basis for the different local anesthetic affinities of resting versus open and inactivated states of the sodium channel. *Mol Pharmacol* **55**:134–141.
- Matsubara T, Clarkson C, and Hondeghem L (1987) Lidocaine blocks open and inactivated cardiac sodium channels. *Naunyn-Schmiedeberg's Arch Pharmacol* **336**:224–231.
- Matsuki N, Quandt FN, Ten Eick RE, and Yeh JZ (1984) Characterization of the block of sodium channels by phenytoin in mouse neuroblastoma cells. *J Pharmacol Exp Ther* **228**:523–530.
- Nuss HB, Balser JR, Orias DW, Lawrence JH, Tomaselli GF, and Marban E (1996) Coupling between fast and slow inactivation revealed by analysis of a point mutation (F1304Q) in m1 rat skeletal muscle sodium channels. *J Physiol* **494**:411–429.
- Ogata N and Narahashi T (1989) Block of sodium channels by psychotropic drugs in single guinea-pig cardiac myocytes. *Br J Pharmacol* **97**:905–913.
- Quandt FN (1988) Modification of slow inactivation of single sodium channels by phenytoin in neuroblastoma cells. *Mol Pharmacol* **34**:557–565.
- Ragsdale DS, McPhee JC, Scheuer T, and Catterall WA (1994) Molecular determinants of state-dependent block of Na<sup>+</sup> channels by local anesthetics. *Science (Wash DC)* **265**:1724–1728.
- Ragsdale DS, McPhee JC, Scheuer T, and Catterall WA (1996) Common molecular determinants of local anesthetic, antiarrhythmic and anticonvulsant block of voltage-gated Na<sup>+</sup> channels. *Proc Natl Acad Sci USA* **93**:9270–9275.
- Schain RJ, Ward JW, and Guthrie D (1977) Carbamazepine as an anticonvulsant in children. *Neurology* **27**:476–480.
- Schauf CL, Penczek TL, and Davis FA (1976) Slow sodium channel inactivation in Myxococcus axons: evidence for a second inactivated state. *Biophys J* **16**:772–778.
- Tomaselli GF, Chiamvimonvat N, Nuss HB, Balser JR, Perez-Garcia MT, Xu RH, Orias DW, Backx PH, and Marban E (1995) A mutation in the pore of the sodium channel alters gating. *Biophys J* **68**:1814–1827.
- Vedantham V and Cannon SC (1999) The position of the fast-inactivation gate during lidocaine block of voltage-gated Na<sup>+</sup> channels. *J Gen Physiol* **113**:7–16.
- West JW, Patton DE, Scheuer T, Wang Y, Goldin AL, and Catterall WA (1992) A cluster of hydrophobic amino acid residues required for fast Na<sup>+</sup> channel inactivation. *Proc Natl Acad Sci USA* **89**:10910–10914.
- Xie XM, Lancaster B, Peakman T, and Garthwaite J (1995) Interaction of the antiepileptic drug lamotrigine with recombinant rat brain type IIA Na<sup>+</sup> channels and with native Na<sup>+</sup> channels in rat hippocampal neurons. *Pflügers Arch Eur J Physiol* **430**:437–446.
- Yang N and Horn R (1995) Evidence for voltage-dependent S4 movement in sodium channels. *Neuron* **15**:213–218.
- Yarov-Yarovoy V, Brown J, Sharp EM, Clare JJ, Scheuer T, and Catterall WA (2001) Molecular determinants of voltage-dependent gating and binding of pore-blocking drugs in transmembrane segment IIIS6 of the Na<sup>+</sup> channel a subunit. *J Biol Chem* **276**:20–27.
- Zimmerman JJ and Feldman S (1989) Physical-chemical properties and biological activity, in *Principles of Medicinal Chemistry*. 3rd ed (Foye WO ed) pp 7–37, Lea & Febiger, Malvern, PA.

**Address correspondence to:** Chung-Chin Kuo, Department of Physiology, National Taiwan University College of Medicine, 1, Jen-Ai Rd., 1st Section, Taipei, 100, Taiwan. E-mail: cckuo@ha.mc.ntu.edu.tw